Planar measurements of velocity and concentration of turbulent mixing in a T-junction

Ingvorsen, Kristian Mark; Meyer, Knud Erik; Nielsen, N. F.

Publication date:
2011

Document Version
Publisher's PDF, also known as Version of record

9TH INTERNATIONAL SYMPOSIUM ON PARTICLE IMAGE VELOCIMETRY - PIV11
Kobe, Japan, July 21-23, 2011

Planar measurements of velocity and concentration of turbulent mixing in a T-junction

K. M. Ingvorsen[1], K. E. Meyer[1], N. F. Nielsen[2]

[1]Department of Mechanical Engineering, Technical University of Denmark, DK-2800 Kgs. Lyngby, Denmark
kmin@mek.dtu.dk, kem@mek.dtu.dk

[2]FLSmidth Airtech, DK-2500 Valby, Denmark
nfn@fls.com

ABSTRACT

Turbulent mixing of two isothermal air streams in a T-junction of square ducts are investigated. Three dimensional velocity fields and turbulent kinetic energy are measured with stereoscopic Particle Image Velocimetry (PIV). The concentration field is obtained with a planar Mie scattering technique using the stereoscopic PIV setup. The concentration measurement method is developed in the present study and the accuracy of the technique is investigated. The resulting data are two dimensional concentration fields taken at 4 Hz. The combination of velocity, turbulence and concentration fields give valuable insight into the mixing process, e.g. by showing large scale flow instabilities. The present technique is well suited for easy testing of mixing devices and for validation of computational models.

1. INTRODUCTION

Mixing of gases is a central subject for many industrial processes. An example is flue gas treatment where typical mixing scenarios are mixing of gases with different temperatures, mixing of flue gas and activated carbon for mercury removal and mixing of flue gas and ammonia for $DeNO_x$ applications. These mixing scenarios all require some kind of injection into a main flue gas duct. Poor mixing can lead to reduced performance or damage of equipment. Strong transient effects and well known mixing dependency on turbulence prediction necessitates high quality experimental data. Furthermore, high quality experimental data can be used for validation of computational fluid dynamics (CFD) models, resulting in reduced costs for design optimization and analysis of mixing scenarios.

The main purpose of the present study is to develop and test a technique, based on a standard PIV setup, that provides reliable measurements of the concentration field. The technique is based on Mie scattering of seeding particles 'marking' the flow and is also known as marker nephelometry (Becker [1]). The complexity of the optical setup is reduced, compared to many previous studies, by relying on reference images of the seeded and unseeded flow when inferring the concentration fields from the particle images. The main advantage of the technique is that it makes it possible to obtain both velocity and concentration fields with the same experimental setup.

2. Experimental Method

2.1 Flow rig

The flow rig used for the experimental investigations is shown in Figure 1. The main inlet is a pipe with a diameter of 245 mm. A transition connects the pipe to a duct with a square cross section with width and height (h) 200 mm × 200 mm. The secondary inlet, mounted perpendicular to the main duct, has a square cross section of 150 × 150 mm. At the entrance of the secondary inlet an adjustable orifice is mounted. The adjustable orifice makes it possible to adjust the flow rate ratio between the main and secondary inlet. Downstream the main duct an orifice plate for the total flow rate is placed. The bulk velocity of the main and secondary inlet are $U_m = 4.0$ m/s and $U_s = 5.8$ m/s, respectively. The Reynolds number based on the main inlet parameters is $Re = U_m h/\nu = 50{,}000$, where ν is the kinematic viscosity of air at 20° C. The flow through the flow rig is driven by a frequency controlled centrifugal fan placed downstream the orifice. The vertical sides of the square ducts are made of transparent acrylic glass, except for the measuring sections where glass is used to increase the quality of the optical access.

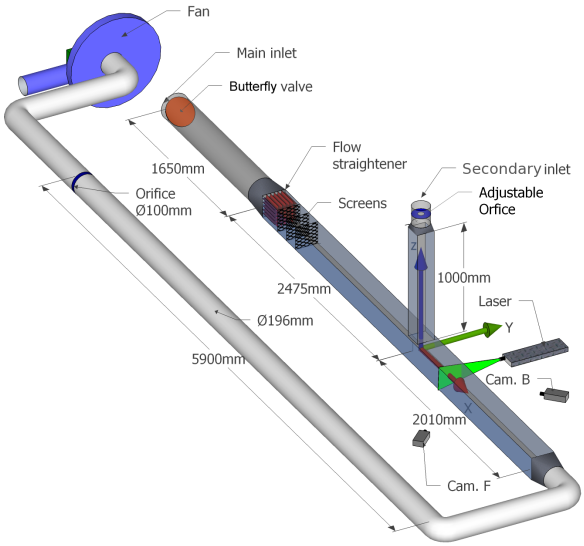

Figure 1: Experimental setup including flow rig and optical system

The seeding particles used for the PIV and concentration measurements are atomized glycerin drops and can be added to both the main and secondary inlet. The Mie scattering technique requires that the seeding particles are well mixed giving a homogeneous concentration of seeding particles in the main flow upstream the T-junction. To promote mixing of the flow and seeding particles added in the main inlet, a mixing device creating large scale vortices (a 45° open butterfly valve) is mounted at the entrance of the main inlet. To obtain a well defined flow in the main duct a flow straightener and three 50% open screens are installed in the entrance of the main duct.

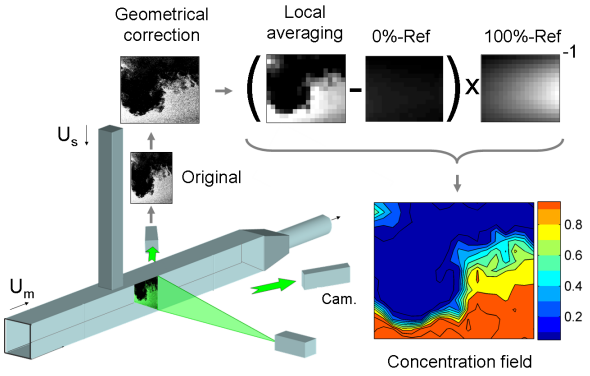

Figure 2: General principle of Mie scattering technique

The flow straightener stops the large scale structures created by the butterfly valve while the screens promote a uniform mean velocity profile.

2.2 *Optical System*

The optical system used for the PIV and concentration measurements is a commercial PIV system consisting of a laser, two cameras and a frame grabber. The optical system is controlled by the Dantec Dynamic Studio version 2.21.2 software and the frame grabber is a National Instruments PCI-1426. The laser is a frequency doubled pulsed Nd:YAG double cavity laser (NewWave solo120xt) with a nominal energy per pulse of 120 mJ. Analysis of uniformly seeded images showed a constant energy per pulse and only limited variations in the intensity profile. The two cameras are 12-bit gray scale digital cameras (Dantec Hi-sense Mk2) mounted with 60 mm Nikon lenses. The CCD chips have a resolution of 1344×1024 pixels and a pixel pitch of $6.45\,\mu$m. The combination of the oblique viewing angle and the rectangular CCD-chip results in an elongated field of view. To account for this, the cameras are rotated 90 degrees such that the 1344 pixel side is vertical.

It is desirable to have a field of view corresponding to the full 200×200 mm duct cross-section. However, reflections from the glass walls makes this very difficult. The maximal achievable measurement area was found to be approximately 160×150 mm. The angle between the cameras is 90 degrees and the angle between the camera and lens is 5 degrees. The cameras are referred to as camera B and camera F (see Figure 1), indicating their backward and forward scatter positions. Due to the angular dependency of Mie scattering, camera F receives significantly more light than camera B. To account for this the f-number on the lens of camera B and F is set to $f_{\#,B} = 5.6$ and $f_{\#,F} = 11$, respectively.

2.3 *Stereoscopic particle image velocimetry (PIV)*

To measure the three-dimensional velocity fields in the main duct a stereoscopic particle image velocimetry system is used. The data processing of the PIV images was carried out using the Dynamic Studio version 2.21.2 software. The particle images were processed to vector fields using an adaptive correlation with interrogation areas of 32×32 pixels and 50% overlap. The mean particle image size at the vertical center line was estimated to be 1 and 2 pixels for camera B and F, respectively.

2.4 *Planar Mie scattering technique*

On Figure 2 the general principle of the Mie scattering technique is illustrated. The figure shows two gas streams being mixed in a T-junction. The flow from the main inlet is marked with a homogeneous concentration of seeding particles while no seeding particles are added to the flow from the secondary inlet. A light sheet is created using a pulsed laser and the camera records the light scattered from the particles in the light sheet. The recorded image is geometrically transformed and a local averaging is carried out. Finally, the image is converted into a concentration field by subtracting and normalizing with reference images corresponding to 0% and 100% concentration, respectively. Only one camera is needed but using two cameras gives the possibility to check the technique. The details of the different steps of the Mie scattering technique will be presented in the following.

As the laser sheet is viewed from an oblique angle the image is distorted and requires a geometrical transformation. This transformation is performed with the PIV-software using the information from the PIV-calibration.

A local area averaging, or binning, is carried out on the geometrically transformed images. The main purpose of this binning is to reduce the noise created by recording an image of randomly positioned particles, the so called marker shot noise. The binning consist of taking a block of $n \times n$ pixels and assigning the mean light intensity to the coordinate corresponding to the center of the block. The binning procedure results in a decrease of the spatial resolution but also in a reduction of data. The reduction in data reduces the processing time significantly. A binning area size of 64×64 pixels is chosen resulting in a spacial resolution of 18×15 points.

By the assumption of a temporal and spatially constant particle size distribution Becker [1] shows that the light scattered from a given binning area is proportional to the number density of the seeding particles. This can be used to convert the recorded light intensity of a given binning area to a corresponding concentration. However, two different binning areas with the same number density will in general not result in the same recorded light intensity. This is the combined result of several different factors influencing the recorded light intensity from a binning area. An overview of the main contributing factors are presented below.

- The light sheet has a non-uniform intensity distribution due to the Gaussian profile of the laser beam.
- The intensity of the scattered light is dependent of the scattering angle as described by Mie theory. Particles located at different positions in the laser sheet will therefore have different scattering efficiencies.
- Non-uniform attenuation of light from the laser to the particles and of the scattered light from the particles to the camera due to imperfections in the optical access through the glass walls.
- Increase in recorded light intensity due to background illumination. The three main sources of background illumination are i) Ambient light from the surroundings. ii) Laser light scattered from permanent objects in the experimental setup. iii) Illumination of background by light scattered from the particles in the light sheet
- Attenuation of the laser beam through the seeded air, so-called laser sheet extinction.
- Attenuation of the light scattered from the particles in the laser sheet by particles occupying the path from the laser sheet to the camera, so-called signal trapping.

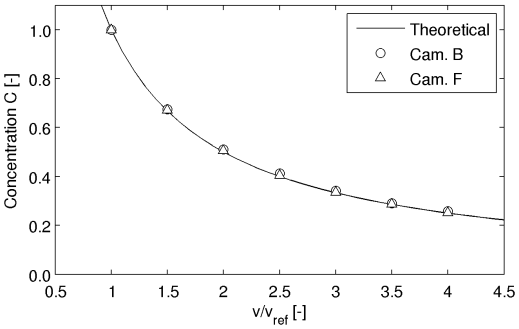

Figure 3: Validation of Mie scattering technique. Comparison of theoretical concentration and concentration measurements based on camera B and F

The contributions from laser sheet extinction and signal trapping becomes important only for high seeding concentrations. A high seeding concentration is defined as an attenuation of the laser light of 5% as it goes through the seeded medium (Shaughnessy and Morton [2]). The attenuation of the laser light was not directly measured, however, a test was carried out using different seeding concentrations indicating that the contributions from laser sheet extinction and signal trapping are negligible at the used concentrations.

The contributions from the beam profile, scattering angle and background illumination from item i) and ii), can be accounted for by using two reference images. One reference image of the unseeded flow $\chi_{uns}(y,z)$ and one reference image of the uniformly seeded flow $\chi_{uni}(y,z)$. χ denotes an images in the form of light intensities in the range of $0-100\%$ corresponding to the 12 bit scale. The reference images χ_{uns} and χ_{uni} are the mean images of their respective series and are based on 25 and 100 images respectively. The reference image of the unseeded flow $\chi_{uns}(y,z)$ corresponds to 0% concentration, while an image corresponding to 100% concentration is obtained by subtracting the unseeded reference image from the uniformly seeded reference image. The instantaneous concentration field $c_i(y,z)$ can now be obtained from the particle image $\chi_i(y,z)$ by subtracting and normalizing with the images corresponding to 0% and 100% concentration.

$$c_i(y,z) = \frac{\chi_i(y,z) - \chi_{uns}(y,z)}{\chi_{uni}(y,z) - \chi_{uns}(y,z)} \tag{1}$$

A test is carried out to investigate the validity of the Mie scattering technique. The secondary inlet is closed and images are recorded of the uniformly seeded flow from the main inlet. The seeding concentration is varied by adjusting the flow rate, while holding the seeding rate constant. Concentration measurements are carried out for eight different concentration levels corresponding to bulk velocities of $U = 2-8$ m/s using the images obtained at $U = 2$ m/s as the 100%-reference. For each concentration level the time averaged concentration field is obtained by recording 100 images. The final estimate of the concentration is obtained by taking the mean of the time averaged concentration field. A plot of the concentration and the Mie scattering concentration measurements are presented in Figure 3.

The plot shows excellent agreement between the concentration and the Mie scattering measurements with a maximum error of 1%. The measurements from camera F are consistently more accurate than measurements from camera B. This is interpreted as the effect of a better S/N ratio caused by the higher light intensities received.

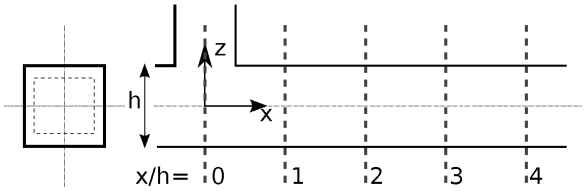

Figure 4: Measuring positions

x/h	$[-]$	0	1	2	3	4
$\langle U_{vw} \rangle$	[m/s]	2.13	0.51	0.35	0.34	0.24

Table 1: Mean in-plane velocity magnitude $\langle U_{vw} \rangle$ for different streamwise positions

The uncertainty of the instantaneous concentration measurements are investigated using the images from the uniformly seeded reference series. The 100 images are converted into concentration fields. The instantaneous concentration should ideally be 1 for the entire field corresponding to 100% concentration. The uncertainty based on an instantaneous concentration estimate is found to be $\pm 12\%$ of the local mean corresponding to a 95% confidence interval. This uncertainty contains contributions from all sources of noise in the experiment but is dominated by the contributions from the suboptimal mixing of seeding particles and the marker shot noise.

3. Results

In this section the results of the velocity and concentration measurements will be presented. The velocity fields u,v,w measured with the PIV-system have a resolution of 83×63 points. The concentration fields measured by the Mie scattering technique have a resolutions of 18×15 points. For both velocity and concentration measurements the sample rate is $f = 4$ Hz, the measuring area is 160×150 mm and measurements are carried out at five streamwise positions $x/h = \{0,1,2,3,4\}$ (see Figure 4).

3.1 Velocity and turbulence

The three-dimensional time averaged velocity fields at the five measuring positions are presented in Figure 5. The velocity fields are plotted in a 200×200 mm box corresponding to the duct size. The vector field at $x/h = 0$ have one scaling (5 m/s corresponds to 25 mm on the axis), while the remaining vector fields have a scaling four times larger. Figure 5 shows that the velocity fields are reasonably symmetric indicating well defined inlet flow. A region with backflow is observed in the top half of the duct. This backflow is caused by a recirculation zone created downstream the T-junction. In addition to the recirculation zone a counter rotating vortex pair (CRVP) is observed. The CRVP is one of the four main flow structures associated with a jet in a cross flow type flows (see e.g. Meyer et al [3]). The CRVP is dominating the transport of the scalar in the mixing process Plesniak and Cusano [4]. For the downstream positions it is observed that the axial velocity becomes more uniform and that the in-plane magnitude magnitude $U_{vw} = \sqrt{\overline{v}^2 + \overline{w}^2}$ rapidly decreases (see Table 1).

The turbulent kinetic energy $k = \frac{1}{2}\left(\overline{u'^2} + \overline{v'^2} + \overline{w'^2}\right)$ is calculated for the different cross-sections (Figure 5, right). At

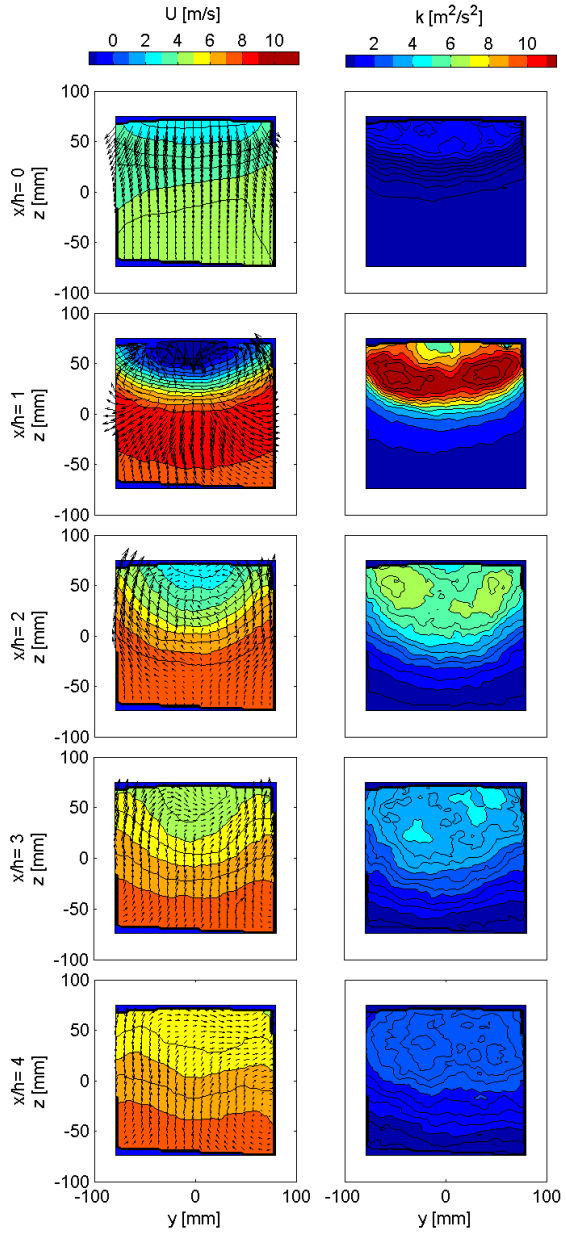

Figure 5: Contour plots of time averaged velocity fields (left) and turbulent kinetic energy (right) for streamwise positions $x/h = \{0,1,2,3,4\}$. The vectors shows the in-plane velocity. Note that the region with zero-values at the boundary of the scalar fields are an artifact of missing data

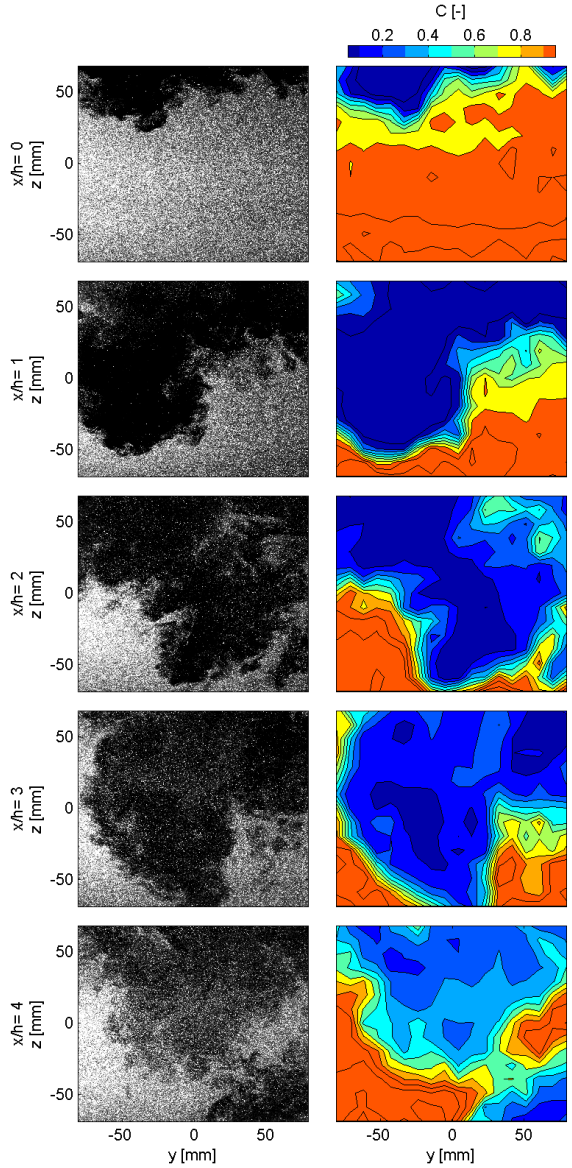

Figure 6: Particle images of mixing (left) and corresponding instantaneous concentration fields (right) for streamwise positions $x/h = \{0,1,2,3,4\}$

$x/h = 1$ high local levels of the turbulent kinetic energy is observed in the region corresponding to the CRVP. For the downstream positions the turbulent kinetic energy is diffused to a larger area of the cross-section resulting in a reduced intensity. For all positions the turbulent kinetic energy is highest in the top half of the duct.

3.2 Concentration

In Figure 6 particle images of mixing and the corresponding instantaneous concentration fields are presented. From the particle images it can be seen that the mixing occurs at small and large scales simultaneously. Furthermore, sharp concentration gradients are observed on the particle images at $x/h = \{0,1,2\}$.

Looking at the particle images from $x/h = 1$ it can be seen that the images can be divided in three regions. A high concentration region bottom of the duct, a region in the middle with zero concentration and a region in the top with a low concentration. This concentration distribution is a result of the CVRP. The

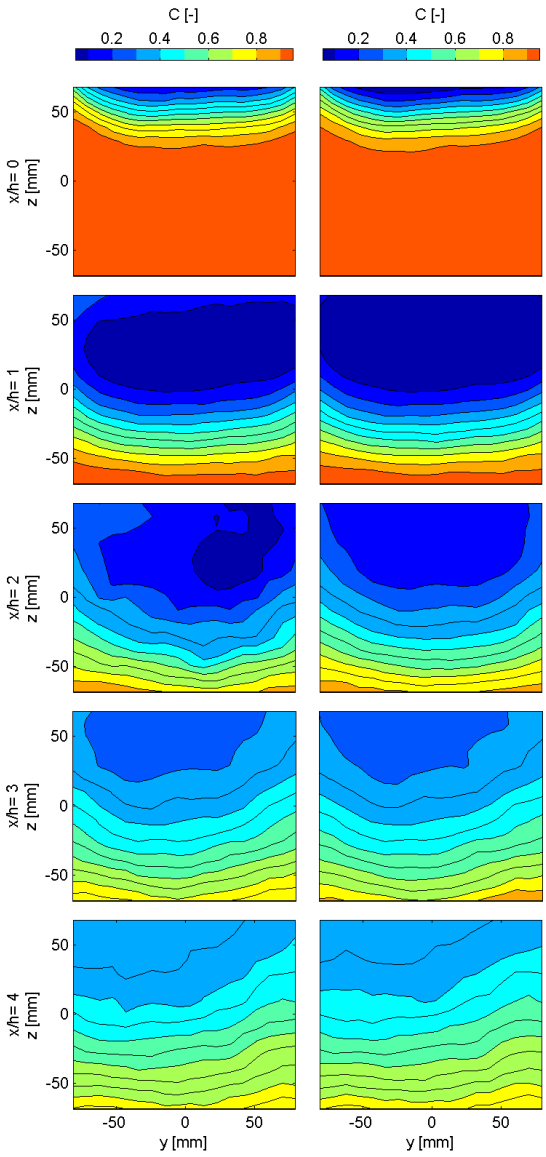

Figure 7: Time averaged concentration fields. (left) Cam. B (right) Cam. F for streamwise positions $x/h = \{0,1,2,3,4\}$

CVRP folds the flow from the main duct around the flow from the secondary inlet resulting in the observed concentration distribution. Finally it is noted that even at $x/h = 4$ regions with concentrations of $10-20\%$ and regions with concentrations of $90-100\%$ still exists.

The time averaged concentration fields, based on 500 samples, for both cameras are shown in Figure 7. The estimates from the two cameras show good agreement. For both cameras the concentration fields are close to symmetric and clearly show the reduction of concentration gradient as a function of the downstream position. The distribution of the scalar on the time averaged concentration field at $x/h = 1$ clearly correlates with the location of the CRVP.

4. Conclusion

In this study turbulent mixing in a generic T-junction geometry with square-cross sections was investigated experimentally. Three velocity components were measured with stereoscopic particle image velocimetry (PIV) and 2D concentrations fields were measured with a planar Mie scattering technique. The Mie scattering technique was developed for the present study and uses the same optical setup as stereoscopic PIV. Further analysis showed a low level of systematic error and random errors corresponding to an uncertainty of $\pm 12\%$ of the local mean on instantaneous concentration measurements. The main sources of uncertainty are the marker shot noise and non-uniformities in the seeding concentration. The uncertainty on instantaneous concentrations is larger than for a corresponding planar laser induced fluorescence (PLIF) measurement. However, the reduced cost of equipment, simpler optical setup and the possibility to do PIV with the same setup may in some experiments make the Mie scattering technique the best choice. The technique was in the validation case shown to give high quality experimental data on the mean concentration distribution. In addition, the method provided quantitative information of the instantaneous concentration fields as well as qualitative information of the mixing process. The technique has a large future potential for providing validation data for CFD simulations of mixing processes as well as testing mixing devices and strategies.

REFERENCES

[1] H. A. Becker, Mixing, concentration fluctuations and marker nephelometery, in: B. E. Launder (Ed.), Studies in Convection, Vol. 2, Academic Press, 1977, pp. 45–139.

[2] E. J. Shaughnessy, J. B. Morton, Laser light-scattering measurements of particle concentration in a turbulent jet, J. Fluid Mech. 80 (1) (1977) 129–148.

[3] K. E. Meyer, J. M. Pedersen, O. Özcan, A turbulent jet in crossflow analyzed with proper orthogonal decomposition, J. Fluid Mech. 583 (2007) 199–227.

[4] M. W. Plesniak, D. M. Cusano, Scalar mixing in a confined rectangular jet in crossflow, J. Fluid Mech. 524 (2005) 1–45.